View metadata, citation and similar papers at core.ac.uk

brought to you by CORE

provided by IntechOpen

We are IntechOpen, the world's leading publisher of Open Access books Built by scientists, for scientists

4,800
Open access books available

122,000
International authors and editors

135M
Downloads

Our authors are among the

154
Countries delivered to

TOP 1%
most cited scientists

12.2%
Contributors from top 500 universities

CLARIVATE ANALYTICS BOOK CITATION INDEX INDEXED

WEB OF SCIENCE™

Selection of our books indexed in the Book Citation Index in Web of Science™ Core Collection (BKCI)

Interested in publishing with us?
Contact book.department@intechopen.com

Numbers displayed above are based on latest data collected.
For more information visit www.intechopen.com

5

Actively Q-switched Thulium Lasers

Jan K. Jabczynski[1], Lukasz Gorajek[1], Waldemar Zendzian[1],
Jacek Kwiatkowski[1], Helena Jelinkova[2], Jan Sulc[2] and Michal Nemec[2]
[1]*Military University of Technology, Warsaw,*
[2]*Czech Technical University, Prague,*
[1]*Poland*
[2]*Czech Republic*

1. Introduction

The near and mid infrared range of optical spectrum (1500 – 5000 nm) has attracted great attention over the last decades, mainly because of a numerous set of absorption / emission lines being "finger prints" of specific chemical and biological compounds (see e.g. (Sorokina & Vodopyanov, 2003)). One of the most reliable techniques for stand alone detection and identification of such agents is laser spectroscopy, for which the coherent, highly monochromatic, tuneable laser sources are required. Research on mid infrared laser sources destined for long range detection is one of the most active areas of solid state photonics nowadays (see e.g. (Godard, 2007) (Mirov et al., 2007) etc.) (Schellhorn, et al., 2007) (Eichhorn, 2008)). One of the necessary requirements for such application is high spatial coherence of laser output beam (parameter M^2 near 1). Among the most perspective types of lasers operating in a mid infrared range (above 2.2 μm-wavelength) are quantum cascade lasers, Cr^{2+}:$A_{II}B_{VI}$ lasers and optical parametric generators. For shorter wavelengths laser diodes and erbium (1600 – 1700 nm), thulium (1800 - 2000 nm), holmium (2050-2200 nm) solid state lasers realised in bulk/crystalline/ or fibre technology are available. The main properties differentiating such groups of lasers are peak power and pulse energy. It has to be pointed out, that for such a wavelength range, damage thresholds of optical elements are severely decreased, comparing to 1-μm wavelength, because of the presence of water vapour and OH groups, having a wide absorption peak just in this wavelength range. The physics of laser action in semiconductor lasers prohibits the high peak power and high energy operation. Moreover, the high CW power 1D or 2D laser diodes stacks characterise low spatial coherence and high beam volume, thus they can be used mainly as optical pumps for other lasers, e.g. holmium or erbium ones.

For short infrared range (< 2 μm wavelength) the Tm or Ho–doped fibre lasers sources operating in a CW regime seem to be the most perspective choice (Gapontsev et al., 2007) (McComb et al., 2009). The pulsed operation of fibre lasers, with energies of tens to hundreds of microJoules, can be realized applying Q-switching technique (Eichhorn & Jackson, 2008) (Eichhorn & Jackson, 2009) or gain-switched method. The best result of 2-μm Q-switched Tm:fibre lasers from the point of view of pulse energy (0.6 mJ for 10 Hz of rep. rate) were obtained (Barnes & De Young, 2009). Mid infrared fibre lasers suffer from lack of good quality active glasses and problems with high peak power / high energy operation for

Source: Advances in Solid-State Lasers: Development and Applications, Book edited by: Mikhail Grishin,
ISBN 978-953-7619-80-0, pp. 630, February 2010, INTECH, Croatia, downloaded from SCIYO.COM

longer wavelengths. However the promising result namely 10 W at 2.78-μm-wavelength has been demonstrated recently in the ZBLAN fibre laser (Zhu & Jain, 2007).
Solid state lasers based on bulk crystalline gain media offer much higher peak powers and pulse energies compared to fibre ones. For the shortest wavelengths (1600-1700 nm) the best configuration is an erbium doped crystalline laser pumped by erbium fibre laser (Clarkson et al., 2006) or directly by laser diode (Setzler et al., 2005) (Kudryashov et al., 2009), (Eichhorn, 2008). For 1800-2000 nm wavelength range the thulium doped crystalline laser pumped by laser diodes seems to be the best option (Honea et al.,1997) (Budni et al., 2000), (Dergachev et al., 2002) (So et al, 2006), (Schellhorn, 2008), (Schellhorn et al., 2009). Intensive research has been devoted to thulium doped gain media (see e.g. (Huber et al.,1988) (Payne et al., 1992) (Lisiecki et al.,2006)) and methods of Q-switching. Passive Q-switching by means of holmium or chromium doped saturable absorbers as well as special types of quantum dots structures (Gaponenko et al., 2008) were examined, however simple, active Q-switching by means of acousto-optic modulators seems to be the better choice because of matured technology, very low insertion losses and relatively high damage thresholds.
The aim of this work was the theoretical analysis of such laser types and its experimental verification for one type of gain medium namely thulium doped yttrium, lithium fluoride (Tm:YLF).

2. Theoretical analysis of actively Q-switched thulium lasers

2.1 Model of quasi- three -level laser for CW pumping

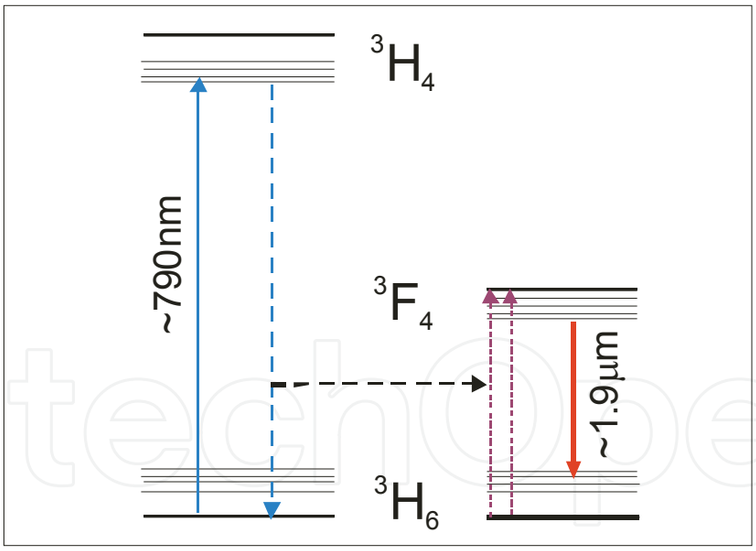

Fig. 1. Scheme of energetic levels of Tm^{3+} gain medium.

The following analysis can be applied to any quasi-three-level laser for which the lower laser levels are partly occupied at room temperature (see e.g. (Beach, 1996) (Bourdet, 2000) (Bourdet, 2001) (Lim & Izawa, 2002)). Typical configuration of Tm^{3+} lasers levels (see Fig. 1) consists of at least three manifolds : $^3H_6$ - pumping and laser lower levels manifold, $^3H_4$ – pumping, upper levels manifold and $^3F_4$ - laser upper level manifold. The pumping process between $^3H_6$ → $^3H_4$, corresponds to wavelength ~ 790 nm which is avaiable for typical AlGaAs laser diodes. Excitation of upper laser levels $^3F_4$ is a result of an efficent cross-

relaxation process $^3H_4 + {}^3H_6 \rightarrow 2 \times {}^3F_4$. In the following analysis we assumed, that this two-stage pumping process is characterised by the quantum efficiency equal to 2. Further, we will consider only relaxation/excitation processes (typical for quasi-III-level lasers) between two manifolds $^3H_6$ - lower pump/laser manifold and $^3F_4$ - upper pump/laser manifold. The analysis given in this paper will be followed by the model developed by (Bourdet, 2000).
Primarily, let us define processes of pumping between lower pumping level of number $N_{p,lower}$ – and the upper pumping level of number $N_{p,upper}$ ($N_{p,lower} \rightarrow N_{p,upper}$). Similarly, the laser transition has to be defined between the pair of levels $N_{l,upper}$ and $N_{l,lower}$ ($N_{l,upper} \rightarrow N_{l,lower}$). It was assumed, that it is valid plane wave approximation and both pump and laser beams have the same radius W and area $A_m=A_p=\pi W^2/2$. For such assumptions the analytical formulae describing the quasi-three-level laser can be derived (see details (Bourdet, 2000)).

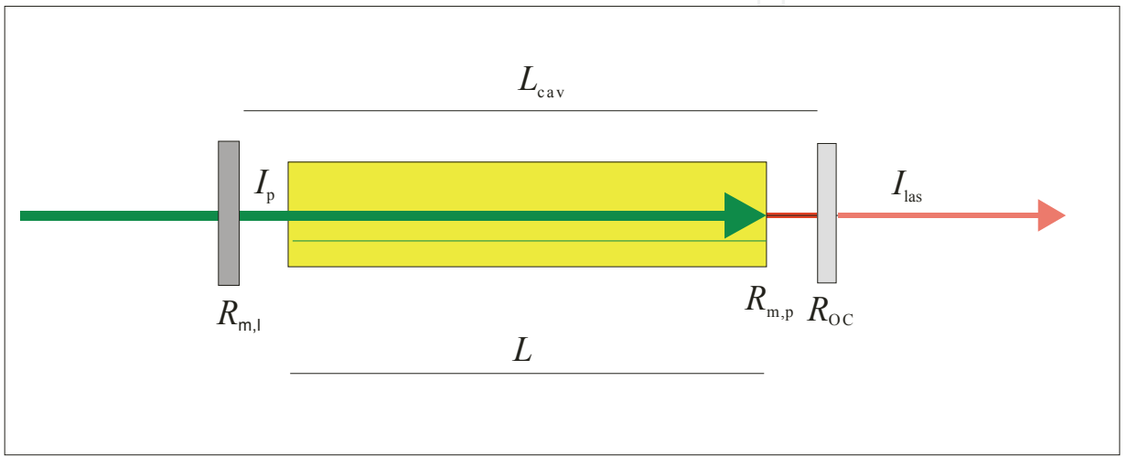

Fig. 2. Scheme of pumping and laser action in the Bourdet's model.

The final expression for relative laser output intensity I_{las} in dependence on incident relative pump intensity I_p and cavity and gain medium parameters is the following:

$$I_{las} = \left(1 - R_{OC}\right)\sqrt{R_{m,l}}\,\frac{\gamma_0 L\left(\dfrac{I_p\left(1-\Gamma\right)\left(1+R_{m,p}\Gamma\right)}{\alpha_0 L} - f_l\right) + \ln\sqrt{R_{OC}R_{m,l}}}{\left(1-\sqrt{R_{m,l}R_{OC}}\right)\left(\sqrt{R_{m,l}}+\sqrt{R_{OC}}\right)}\,, \tag{1}$$

where: L – rod length, $R_{m,l}$, R_{OC} - rear and output mirror reflectivity at laser wavelength, $R_{m,p}$ - rod reflectivity at pump wavelength. The function Γ (corresponding to the transmission of pump beam for laser action) is given by:

$$\Gamma = \left(R_{m,l}R_{OC}\right)^{\alpha_0/2\gamma_0}\exp\left[-\alpha_0\left(f_p - f_l\right)L\right], \tag{2}$$

where:

$$\alpha_0 = \sigma_p N_0\left(f_{N_{p,lower}} + f_{N_{p,upper}}\right) \quad , \quad \gamma_0 = \sigma_l N_0\left(f_{N_{l,lower}} + f_{N_{l,upper}}\right),$$
$$f_p = \frac{f_{N_{p,lower}}}{f_{N_{p,lower}} + f_{N_{p,upper}}} \quad , \quad f_l = \frac{f_{N_{l,lower}}}{f_{N_{l,lower}} + f_{N_{l,upper}}}\,, \tag{3}$$

N_0 – concentration of active ions, σ_p, σ_l – absorption/emission cross sections at pump/emission wavelengths, respectively, f_N – Boltzmann's occupation factor of N–th level. To calculate the final output laser power P_{out} and the incident pump power P_p the relative intensities I_{las}, I_p have to be multiplied by the mode/pump area $A_m = A_p = A = \pi W^2/2$ and emission/ absorption saturation densities $I_{sat,l}$, $I_{sat,p}$ as follows:

$$P_{out} = A\, I_{las} I_{sat,l} \quad ; \quad P_p = A\, I_p I_{sat,p}\,, \tag{4}$$

where:

$$I_{sat,l} = \frac{h\nu_l}{\left(f_{N_{l,lower}} + f_{N_{l,upper}}\right)\tau_u \sigma_l} \quad , \quad I_{sat,p} = \frac{h\nu_p}{\left(f_{N_{p,lower}} + f_{N_{p,upper}}\right)\tau_u \sigma_p} \quad , \tag{5}$$

τ_u- life time of upper laser level , $\nu_p = c/\lambda_p$, $\nu_l = c/\lambda_l$ – pump / laser frequencies, λ_p , λ_l- pump laser wavelengths, c- light speed, h –Planck constant.

Let us summarise the main properties of the quasi-three-level laser:

- strong dependence on temperature via Boltzmann's occupation factors f_N occuring in all formulae
- occurrence of additional, reabsorption losses per roundtrip defined by:

$$\gamma_{reab} = 2\gamma_0 f_l L \tag{6}$$

- minimal pump power required for achieving gain medium transparency:

$$P_{p,min} = \beta_{min} A_p I_{sat,p} \quad , \quad \beta_{min} = \frac{f_l}{f_p - f_l} \quad . \tag{7}$$

Moreover, in contrast to the typical case of a four-level laser, the absorption efficiency is different in laser and non-laser conditions. As a result of laser transition the occupations of upper and lower laser level are "clamped" to those at threshold and are dependent only on coupling conditions, losses etc.

For the case of laser action (above threshold) the absorption efficiency is given by:

$$\eta_{abs,las} = \frac{I_{p,abs}}{I_p} = \left(1 - \Gamma\right)\left(1 + R_{m,p}\Gamma\right) \quad . \tag{8}$$

As a rule, $\eta_{abs,las}$ is higher compared to non-laser conditions and does not depend on pump power.

In the case of non-lasing conditions the main effect of the diminishing of absorption efficiency consists in saturated absorption. Therefore, the absorption efficiency can be defined in two alternative ways:

$$\eta_{abs,non-las} = \left(1 - \Gamma_{lambertW}\right)\left(1 + R_{m,p}\Gamma_{lambertW}\right) \quad , \quad \Gamma_{lambertW} = \frac{LambertW\left(I_p \exp\left(-\alpha_0 f_p L\right)\right)}{I_p}\,, \tag{9}$$

where *LambertW*(z) denotes LambertW function (see e.g. (Barry et al, 2000), (Grace, et al, 2001), (Jabczyński et al, 2003)) defined as follows:

$$LambertW(z)\exp\left[LambertW(z)\right]=z \quad . \tag{10}$$

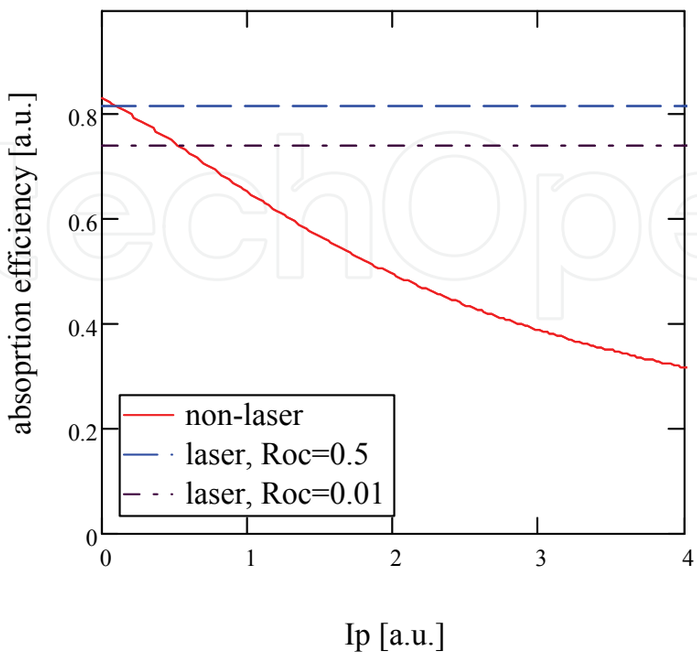

Fig. 5. Absorption efficiency vs. relative pump power; non lasing – continuous curve, lasing R_{oc}=0.5 dotted curve, lasing R_{oc}=0.01 – dash-dot curve.

An alternative way to determine absorption efficiency in non-laser conditions is to find a numerical solution for the pump transmission function Γ of the following equation:

$$\frac{\alpha_o f_p L+\ln\Gamma}{(1-\Gamma)(1+R_{m,p}\Gamma)}=I_p \quad , \tag{11}$$

and substituting the obtained value of Γ to formula (8). The results of absorption efficiency calculation for non-laser and laser conditions are shown in Fig. 5.
Below threshold absorption efficiency decreases with pump intensity. In a laser condition above threshold, absorption efficiency does not depend on pump power and it can even jump to higher values depending on output coupler reflectivity as was shown in Fig. 5. In our case of an actively Q-switched laser the non-lasing condition has to be assumed during the pumping process.

2.1.1 Optimisation of laser parameters

Analysing the formula (1), it is quite easy to find the condition for the optimum length of gain medium. Please note, that the small signal gain (assuming $R_{m,p}$ = 0) can be defined as follows:

$$g_{ss}=\gamma_0\left(\frac{I_p(1-\Gamma)}{\alpha_0 L}-f_l\right). \tag{12}$$

Thus, assuming constant I_p, R_{oc}, $R_{m,p}$, N_o and temperature, after differentiating (12) with respect to L, the final formula on optimal crystal length can be found:

$$L_{\text{opt}} = \frac{\beta_{\min}}{\alpha_0 f_1} \ln\left[\left(R_{m,p} R_{OC} \right)^{\frac{1}{2\gamma_0}} \left(\frac{\beta_{\min}}{I_{\text{p}}} \right)^{\frac{1}{\alpha_0}} \right]. \tag{13}$$

The example of calculation of optimal crystal length dependent on pump intensity is shown in Fig. 6.

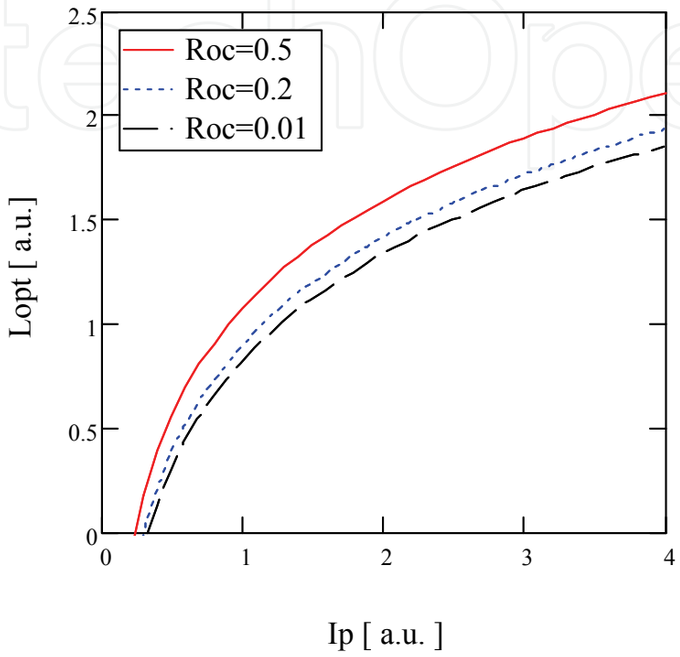

Fig. 6. Optimal crystal length vs. relative pump intensity for different output coupler reflectivities R_{oc}, $R_{\text{m,l}}$=0.99.

Please note, that output power for a given pump intensity depends also on output coupler reflectivity and cavity losses. The typical characteristics of output power intensity vs. pump power intensity are shown in Fig. 7.

As was shown in Fig. 6, 7, to obtain the higher output power with increased pump power density the gain medium length and out-coupling losses have to be increased. Please note that threshold pump power is also the function of gain medium length via reabsorption losses.

In the process of optimisation of quasi-three-level laser parameters, the starting point is the available pump power. We have to find the best combination of pump area, output coupler transmission, gain medium length to obtain the maximum output power. Further, the cavity design (curvature of mirrors, distances) should satisfy the best mode matching condition i.e. the fundamental laser mode area has to be comparable to the pump area to minimize the aperture/absorption losses occurring in an un-pumped region. The above presented formulae can give only preliminary indications, all these rules have to be verified experimentally.

It should be noted, that with increase in pump power density, the temperature of the rod increases, causing an increase in reabsorption losses and additional cavity losses as a result of stress induced aberrations. Thus, it is a trade of between requirements for efficient pumping and thermal limitations of a quasi-three-level laser. In practice, output power of such a laser is limited by thermo-optic effects and thermal fracture (see e.g. (So et al, 2006)),

so the proper choice of pump geometry, size and dopant level of gain medium is fundamental to mitigate these effects.

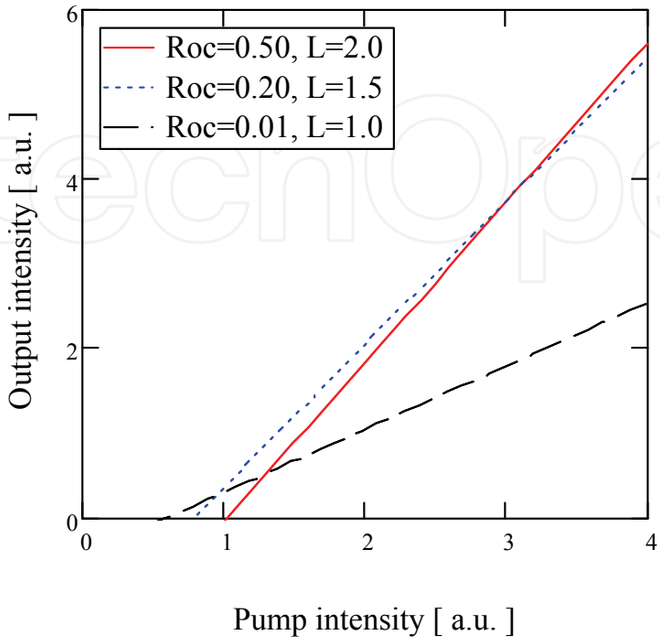

Fig. 7. Output intensity vs. pump intensity.

2.2 The thermo-optic limitations of thulium lasers

For lasers operating in a free running regime the maximum pump power with respect to fracture limit is determined by the doping level and mechanical toughness of the crystal (see e.g. (Koechner, 1996), (Chen, 1999), (So et al, 2006)). Much below fracture limit the operating parameters of any type of diode pumped lasers are governed by the temperature increase inside the gain medium. The temperature profile induced by absorption of a focused pumping beam inside the gain medium of a quasi-three-level laser manifests by means the following effects:

- changes in absorption efficiency and available net inversion,
- reabsorption losses due to temperature dependent occupations of lower laser level,
- paraxial thermal lensing,
- higher order thermal aberration,
- stress induced birefringence and depolarisation losses
- thermal fracture for higher heat loads.

According to the model derived for end pumped lasers (Chen, 1999) the maximum absorbed pump power is given by:

$$P_{\mathrm{abs,lim}} = \frac{4\pi R_{\mathrm{T}}}{\alpha_{\mathrm{abs}} \eta_{\mathrm{h}}}, \tag{14}$$

where: η_{h} – heat conversion efficiency, α_{abs} – absorption coefficient, R_{T} – thermal shock parameter defined, as follows:

$$R_T = \frac{K_c \sigma_{max,fracture}}{\alpha_T E}, \quad (15)$$

where : $\sigma_{max,fracture}$ – fracture limit stress, E – Young's modulus, K_c- thermal conductivity, α_T – linear thermal expansion coefficient.
Assuming top-hat distribution of the pump beam, maximum temperature increase on the z- distance on the axis of the laser rod is given by (Chen, 1999):

$$\Delta T_{max}(z) = \left(1 + \ln\left(\frac{\left(a/W_{p,0}\right)^2}{1+\left((z-z_w)/z_p\right)^2}\right)\right)\frac{\eta_h \alpha_{abs}\exp(-\alpha_{abs} z)}{4\pi K_c\left(1-\exp(-\alpha_{abs} L)\right)}P_{abs}, \quad (16)$$

where : a – rod radius, $W_{p,0}$ – radius of pump beam in the waist, z_w – waist distance to the rod facet, z_p – Rayleigh range of pump beam, P_{abs}- absorbed pump power. To obtain average temperature in the rod, $\Delta T_{max}(z)$ has to be integrated along the rod.
Maximal thermally induced stress inside the rod occurs on rod facet (z=0). Assuming a linear thermal elasticity model, the maximum stress can be estimated by the following formulae:

$$\sigma_{max} = \alpha_T \Delta T_{max}(0) E \quad . \quad (17)$$

For top-hat heat source distribution inside the cylindrical rod we have a parabolic profile of temperature resulting in optical path difference of a parabolic shape. In the framework of a paraxial thermal lensing model, the thermo-optic optical power induced inside the rod is given by:

	Tm:YAG	Tm:$YAlO_3$	Tm:YLF	Tm:YVO_4
Absoprtion peak wavelength [nm]	785	795	792	801
absorption coeff. α_{abs} [cm^{-1}] @1%Tm	1.05	0.9/0.8	0.36	7
Refractive index n	1.81	1.929/1.943	1.47/1.448	1.98/2.16
Temperature dispersion dn/dT [10^{-6}/K]	7.3	9.7	-4.4/-2	8.5/3.9
thermal expansion coefficient α_T[10^{-6}/K]	7.5	10.8	13.3	4.4/11.4
thermal conductivity K_c [W/m/K]	13	11	7.2	11
Young modulus E [GPa]	310	220	85	77
fracture stress $\sigma_{max,fracture}$ [kG/mm^2]	16	16	4	4
Thermal shock parameter R_T [W/cm]	6.5	5.5	1.7	6.1
β_T [mm^2/W/m]	1.17	1.96	0.47	1.71
f_T [mm] @ I_h=1 W/mm^2	85.4	50.8	212.8	58.5

Table 1. Mechanical and optical parameters of 4 typical Tm doped gain media.

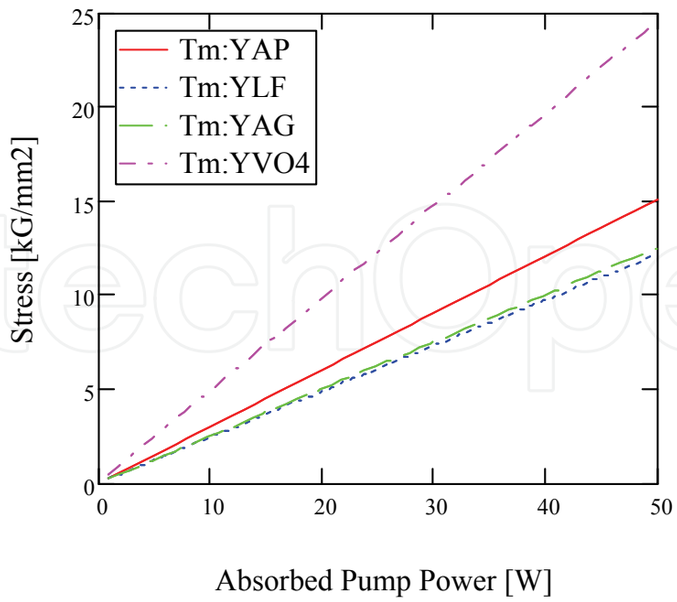

Fig. 8. Maximal stress vs. absorbed pump power for 4 Tm crystals; $W_{p,0}$=0.5mm.

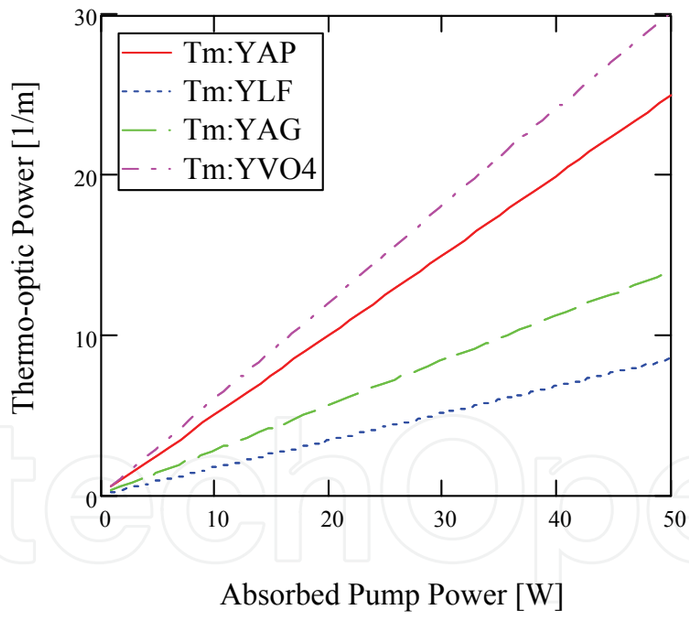

Fig. 9. Thermo-optic power vs. absorbed pump power for 4 Tm crystals; $W_{p,0}$=0.5mm.

$$M_T = f_T^{-1} = \beta_T I_h \quad , \tag{18}$$

where: β_T – thermal lensing parameter, I_h – heat power density defined as follows:

$$\beta_T = \frac{\frac{dn}{dT} + (n-1)(1+\nu)\alpha_T}{K_c} \quad , \quad I_h = \frac{\eta_h P_{abs}}{A_p} \quad , \tag{19}$$

where: ν- Poisson's ration, A_p – averaged pump area, n – refractive index, dn/dT – temperature dispersion of refractive index.
To help in the choice of a proper gain medium for the thulium laser, the mechanical and optical parameters of four Tm-doped media were collected in Table 1.
We have calculated the maximum stress and thermo-optical power vs. absorbed pump power for these 4 gain media (see Fig. 8, 9 respectively).

2.3 Model of actively Q-switched Tm laser
2.3.1 Degnan's analytical model
To analyse the regime of active, periodic Q-switching we can modify the classical models of Q-switching (see e.g. (Degnan, 1989), (Koechner, 1996), (Eichhorn, 2008)). The model of rate equations for a quasi-three-level laser is defined by two functions: Φ – relative intensity of the laser field, and X - modified relative occupation (further called inversion) of the upper laser level:

$$X = X_u - f_l, \tag{20}$$

where f_l –relative occupation of the lower laser level defined by the formula (3).
The set of rate equations consist of two first order differential equations with respect to relative time $\tau = ct/2L_{cav}$ as follows:

$$\begin{cases} \dfrac{d\Phi}{d\tau} = \Phi\left(2\gamma_0 L X - \rho_{cav}\right) \\ \dfrac{dX}{d\tau} = -2\gamma_0 L_{cav}\Phi X - \dfrac{X}{\tau_{rel,u}} + \eta_{abs}\dfrac{I_p}{I_{p,0}} + \dfrac{f_l}{\tau_{rel,u}} + \ldots \end{cases}, \tag{21}$$

where: L_{cav} – length of cavity , $\tau_{rel,u} = c\tau_u/2L_{cav}$ – relative upper level lifetime, I_p – relative pump density,

$$I_{p,0} = \alpha_0 L / \eta_{quant}\ , \tag{22}$$

$$\rho_{cav} = -\ln\left(R_{m,l}R_{OC}\right) + \rho_{on,off}\quad , \tag{23}$$

η_{abs}- absorption efficiency, $\rho_{on,off}$ – losses of active Q-switch, different in pumping and pulsing intervals,

$$\rho_{on,off} = \begin{cases} \rho_{qsw,low} \text{ for } \quad \mathrm{mod}(t, t_{rep}) < t_{off} \\ \rho_{qsw,high} \text{ for } \quad t_{off} < \mathrm{mod}(t, t_{rep}) < t_{on} \end{cases}. \tag{24}$$

The pumping process is periodic with a repetition rate of $f_{rep} = 1/t_{rep}$. In pumping time $t_{on} \approx t_{rep}$, losses of q-switch $\rho_{qsw,high}$ have to be sufficiently high to prevent laser oscillation. In a short interval of duration $t_{off} << t_{on}$, t_{rep} the cavity losses are small and the pulse starts to build up.
For the steady state (after a few initial pulses) the initial inversion X_i before the pulse and final inversion X_f tend to values defined only by pump density, cavity parameters and the repetition period.
We can define threshold inversion for low losses of Q-switch as follows:

$$X_{thr} = \frac{-\ln(R_{m,l}R_{OC}) + \rho_{qsw,low}}{2\gamma_0 L}. \tag{25}$$

To obtain effective Q-switching, pump intensity and duration should be sufficiently high to achieve initial inversion X_{in} a much higher value than X_{thr}:

$$X_{thr} < X_{in} < \frac{-\ln(R_{m,l}R_{OC}) + \rho_{qsw,high}}{2\gamma_0 L}. \tag{26}$$

In pumping time the laser intensity disappears ($\Phi = 0$) and the second equation can be solved analytically, assuming, that absorption efficiency does not change during pumping and other non-linear processes (up-conversion, amplified spontaneous emission) can be neglected. The formula for inversion is the following:

$$X(\tau) = X_\infty - (X_\infty - X(0))\exp(-\tau/\tau_{rel,u}), \tag{27}$$

where: X_∞– inversion achieved for time $\tau >> \tau_{rel,u}$ defined as follows:

$$X_\infty = \tau_{rel,u}\eta_{abs}(I_p)\frac{I_p}{I_{p,0}} + f_l, \tag{28}$$

$X(0) = X_f$ – inversion at the starting point of pumping corresponding to the final inversion after pulse generation. The examples of temporal dependence of inversion for different repetition rates are shown in Fig. 10.

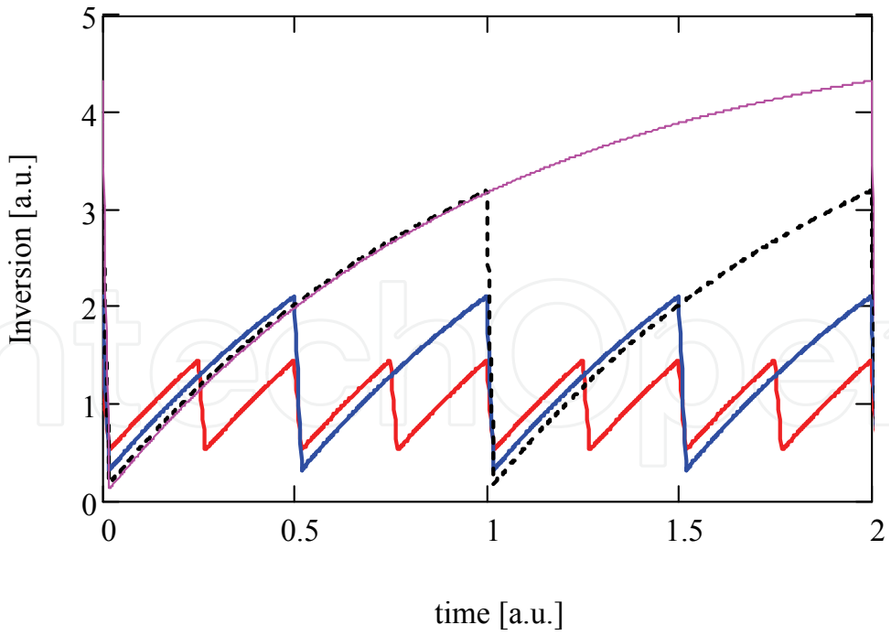

Fig. 10. Changes in inversion vs. time for different repetition periods.

During the pulse build up interval the pumping and relaxation components can be neglected in a second rate equation. Thus, we can find the analytical solution of rate equations in the form of a transcendent equation on initial and final inversions X_i , X_f:

$$\frac{X_f}{X_i} = \exp\left(-\frac{X_i - X_f}{X_{thr}}\right). \tag{29}$$

Using (27), initial inversion can be written as:

$$X_i = X_\infty \frac{1-\exp\left(-\tau_{rep}/\tau_{rel,u}\right)}{1-\exp\left(-\tau_{rep}/\tau_{rel,u}\right)\exp\left(-\left(X_i - X_f\right)/X_{thr}\right)}. \tag{30}$$

To determine the initial inversion including the cross-relaxation and up-conversion processes the more complicated model of a quasi-three-level laser (Rustad & Stenersen, 1996) can be used.

The pulse duration, pulse energy, and peak power can be determined knowing the initial and final inversions. The conditions of optimisation of an actively Q-switched laser were found (Degnan, 1989). Let us introduce the un-dimensional parameter z defined as follows:

$$z = X_i(I_p, \tau_{rep}) / X_{thr}. \tag{31}$$

The optimal reflectivity $R_{OC,opt}$ of the output coupler can be determined as follows:

$$R_{OC,opt} = \exp\left[-\rho_{pas}\left(\frac{z-1-\ln z}{\ln z}\right)\right], \tag{32}$$

where ρ_{pas} – passive cavity losses defined as follows:

$$\rho_{pas} = -\ln\left(R_{m,l}\right) + \rho_{qsw,low}. \tag{33}$$

Let us notice, that $R_{OC,opt}$ depends on the pump density and repetition period.

For optimal out-coupling losses the formulae on pulse duration t_{pulse}, extraction efficiency η_{extr} and output energy E_{out} are the following:

$$t_{pulse} = \frac{2L_{cav}}{c\rho_{pas}}\left(\frac{\ln(z)}{z\left[1-a(z)\left(1-\ln(a)\right)\right]}\right) \quad , \quad a(z) = \frac{z-1}{z\ln(z)} \quad , \tag{34}$$

$$\eta_{extr} = 1 - \frac{1+\ln(z)}{z}, \tag{35}$$

$$E_{out} = E_0\left(z-1-\ln(z)\right), \tag{36}$$

where:

$$E_0 \approx \frac{h\nu_l A_m \rho_{pas}}{2\sigma_l}. \tag{37}$$

Such an elegant, simple analytical model can give mainly qualitative information about the properties of the Q-switched laser. It should be underlined the role of parameter z equal to the ratio of small signal gain to passive losses. The quality of laser output is proportional to parameter z which could be determined for any type of laser (including high repetition rate Q-switched fibre lasers as well). The short pulses and high peak powers, evidencing effective Q-switching, occur for z > 10.

However, comparing Degnan's analytical model with experiments, quite large differences can be found especially for high pumping rate and long repetition periods. It should be noted, that in this model all non-linear processes are neglected, whose role is growing with increase in inversion. Moreover, with an increase in heat load the several temperature dependent processes (thermally induced aberration, stress, lowering of gain etc.) significantly diminish the performance of the laser.

2.3.2 Numerical modelling of an actively Q-switched Tm:YLF laser.

Comparing results of theoretical analysis with experiments on the Q-switched Tm:YLF laser, it was found, that it is necessary to improve the model adding the thermo-optic and cavity effects. Therefore, we have developed a numerical model (Gorajek, et al, 2009) introducing additional losses $\gamma_{add}(T)$ occurring as a result of the absorption of laser mode wings on unpumped regions of a quasi-three-level medium. In the particular case of our oscillator, the laser scheme for "cold" cavity is nearly half confocal (g_1=1, g_2 = 0.5) for vanished thermal lensing). With increase in negative thermal lensing (typical for Tm:YLF crystal) the mode size at the crystal increases until reaching the stability limit of the cavity ($g_1 \sim 2$, g_2 =0.5). However, also, even out of stability range, the spatially limited mode is formed due to diffraction on the gain diaphragm induced by the pumping beam, which could be treated as a kind of "imaginary" lens (Grace, et al , 2001) (Jabczyński et al, 2003). Such a laser mode has a "gaussian" like profile and much higher diffraction losses which depend (via temperature increase) on average pump power. To determine the maximal, average temperature in rod and thermal lensing power the analytical formulae (16), (18), (19) were applied. For calculation of the additional losses $\gamma_{add}(T)$ the numerical procedure proposed in (Jabczyński et al, 2003) was used. The results of the calculation of average temperature and pump dependent losses for two cases: quasi-CW pumping (duty factor 10%) and CW pumping are shown in Fig. 11

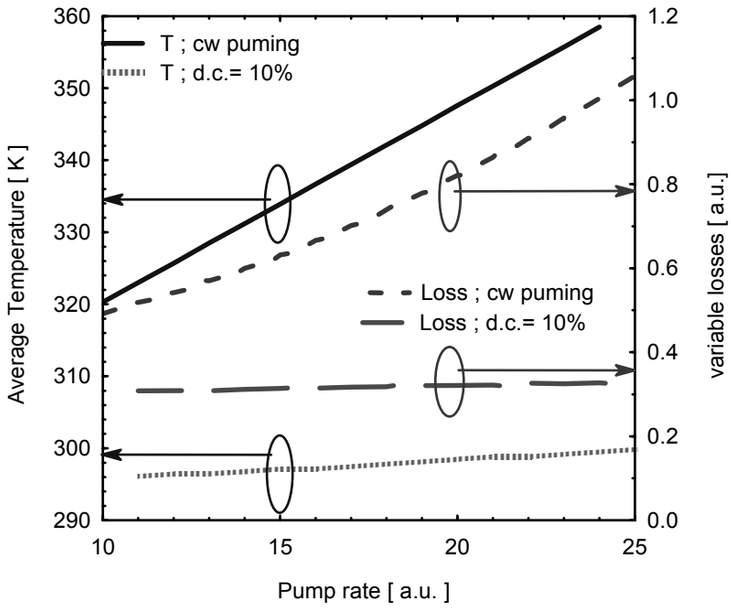

Fig. 11. Average temperature inside rod, pump dependent losses vs. pump rate: CW pumping.

The numerical procedure prepared for analysis of giant pulse formation was divided into two stages. In the first one, before switching off the high Q-switch losses, the internal flux vanishes and only the second equation is numerically solved. Moreover additional non-linear effects causing a drop in inversion can be added. After switching off the Q-switch, the threshold condition is tested and the set of both equations is solved for the giant pulse evolution calculation.

The main difference in analysis of Q-switching in a quasi-three level laser (compared to the four level scheme) consists on the effect of temperature on the available parameters of the giant pulse. Because of the increase in temperature with pump power, the inversion and additional losses significantly influence on the available peak power and pulse duration (see Fig. 12-13).

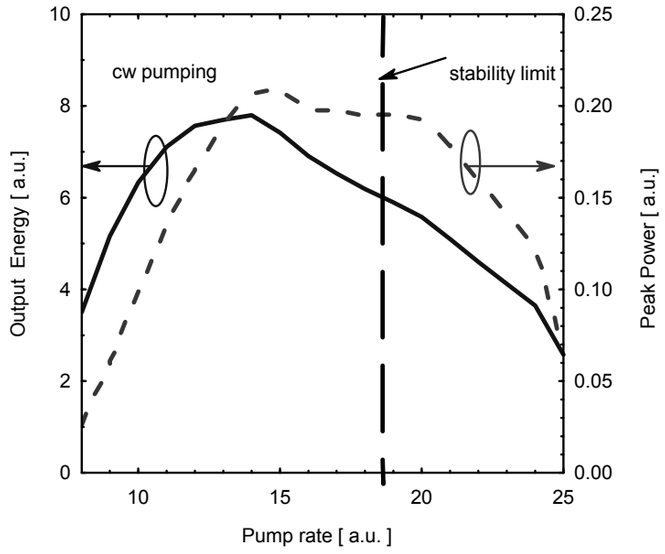

Fig. 12. Average output power, peak power vs. pump rate: CW pumping.

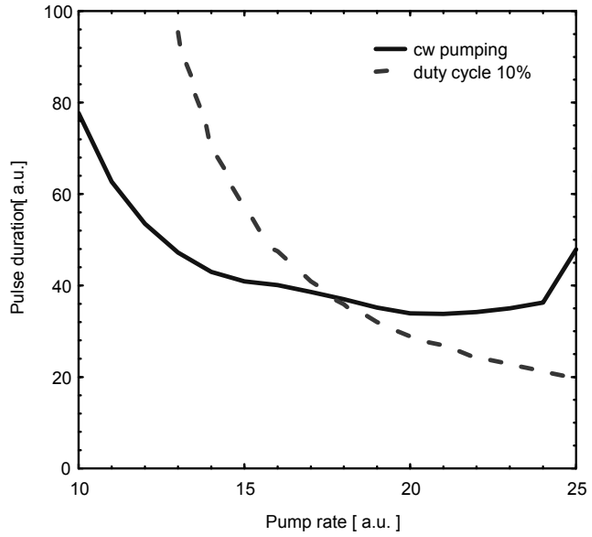

Fig. 13. Pulse duration vs. pump rate; CW pumping continuous curve, pumping duty cycle 10%– dashed curve.

The all above presented effects give the result, that giant pulse is generated for a considerable level of losses dependent on effective average heat power dissipated in the gain medium. Such effects were observed in experiments (see p.3.3 and p.3.4) and we have shown in Fig. 11-13 the results of simulation qualitatively explaining the experiment.

3. Experiments

3.1 Laser head scheme

We have designed the laser head of a diode pumped Tm:YLF laser shown in Fig. 14 destined for tuneable and Q-switched operation (Jabczyński, et al., 2007) (Jabczyński, et al., 2009). The fibre coupled diode of 30-W output power emitting at a 0.792 μm wavelength was deployed as a pump source.

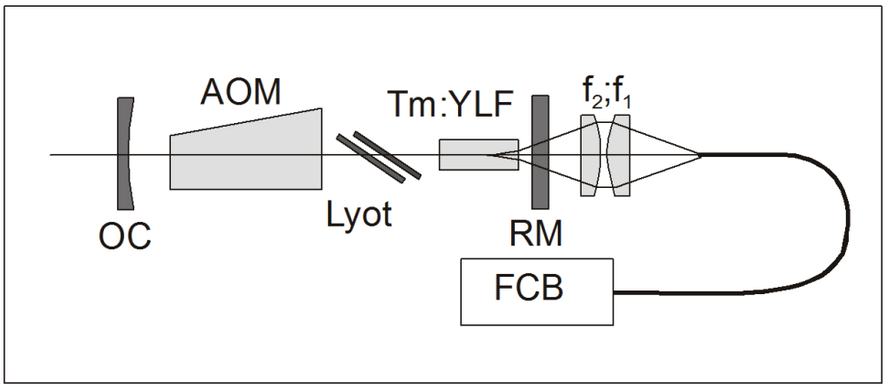

Fig. 14. Optical scheme of a Tm:YLF laser: FCB- fiber coupled laser diode of 30 W, RM- rear flat mirror, OC- output coupler, Tm:YLF- gain crystal, AOM- acousto-optic Q-switch.

The pump beam after passing through a reimaging optic (of 1.5 x magnification) forms inside the gain medium the caustics of waist diameter approximately 0.6 mm and induces a near 60 K increase in temperature for the maximum incident pump power of 26 W.
The uncoated, with 3.5%. doping of thulium YLF rods of 8 and 10 mm size wrapped with indium foil were tested as gain media. The crystals were mounted in a copper heat-sink maintaining 293 K temperature of coolant. The diode wavelength was tuned via the control of thermo-electric cooler voltage to maximise the absorbed pump power, however not higher than 65% absorption efficiency for an 8-mm long rod and 80% for a 10-mm crystal were obtained in the best cases of CW pumping without lasing (see Fig. 15).

3.2 Free running and tunablity characterisation

As the output couplers we have used mirrors of a 0.3 and 0.5 m radii of curvature and 10%, 15%, 20% and 30% transmission at a 1.9-μm wavelength. The energetic characteristics in quasi-CW pumping in dependence on absorbed pump power were presented in Fig. 16.
Above 7-W power with nearly 30% slope efficiency with respect to incident pump power were demonstrated for the best case of quasi-CW pumping for a short, 70-mm resonator. Nearly 5 W were obtained for CW pumping in a short cavity and above 3 W for an elongated 220-mm cavity.

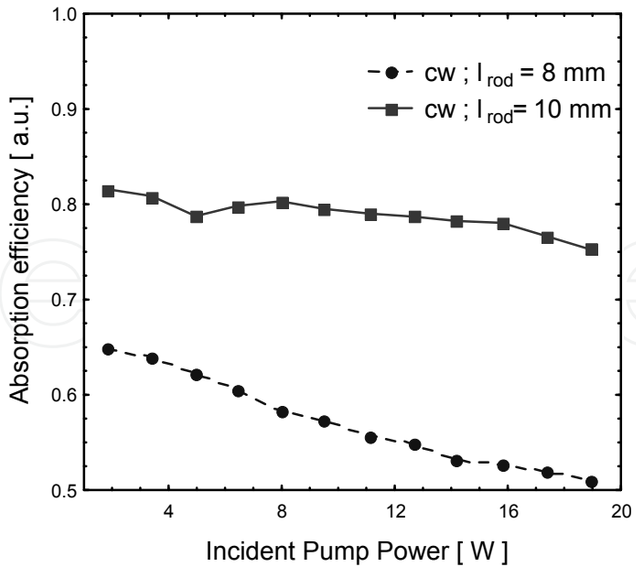

Fig. 15. Absorption efficiency in non-lasing conditions vs. incident pump density for two Tm:YLF rods.

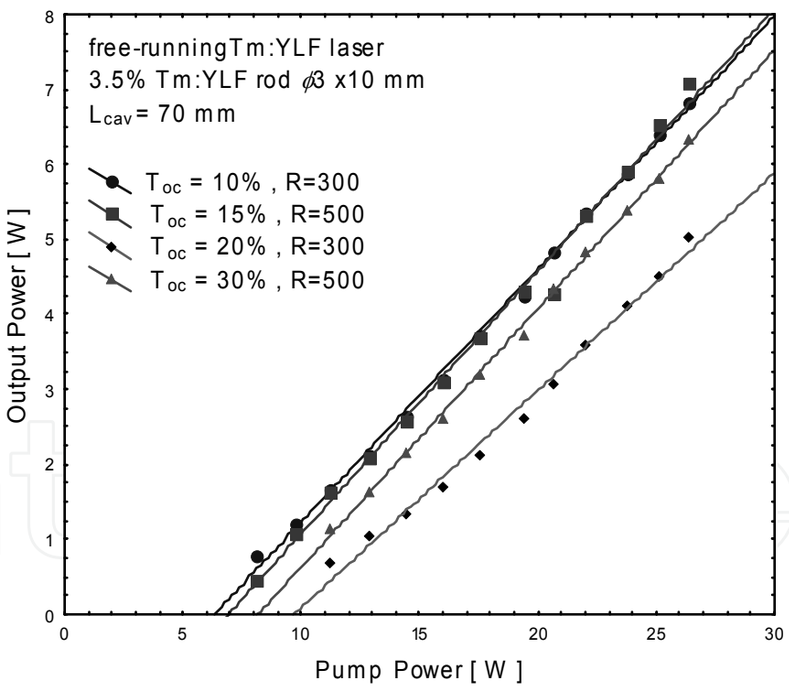

Fig. 16. Output power vs. pump power for quasi-CW pumping (10% duty cycle, 10Hz, 10ms pump duration).

The spectrum of generation was centred at 1908 nm with FWHM of approximately 6 nm (see Fig. 17) for the oscillator without deploying Lyot's filter. In the next step of experiments the cavity was elongated to 220 mm to deploy the Lyot's filter (consisting of 2 quartz plates of 0.92 and 1.84 mm thickness, respectively) and an active Q-switch.

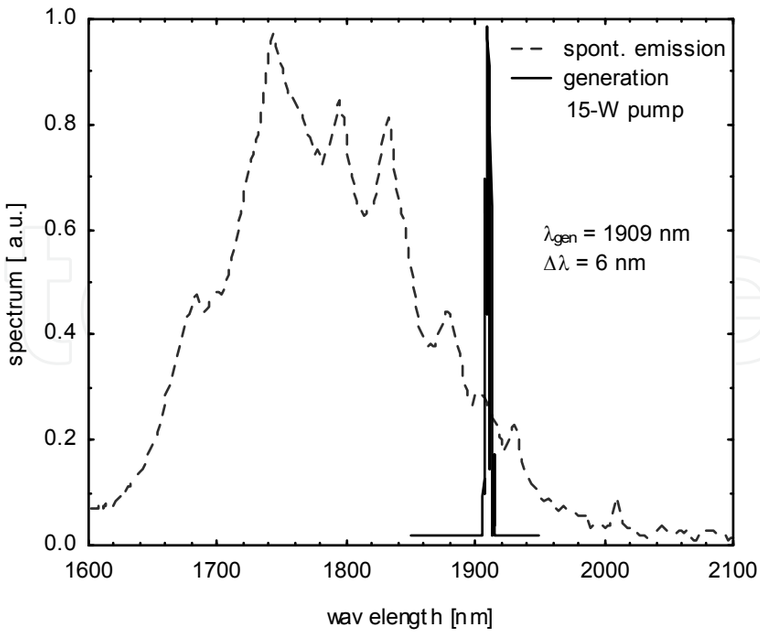

Fig. 17. Spectra of spontaneous emission and free-running of a Tm:YLF laser with 10%- transmission of OC.

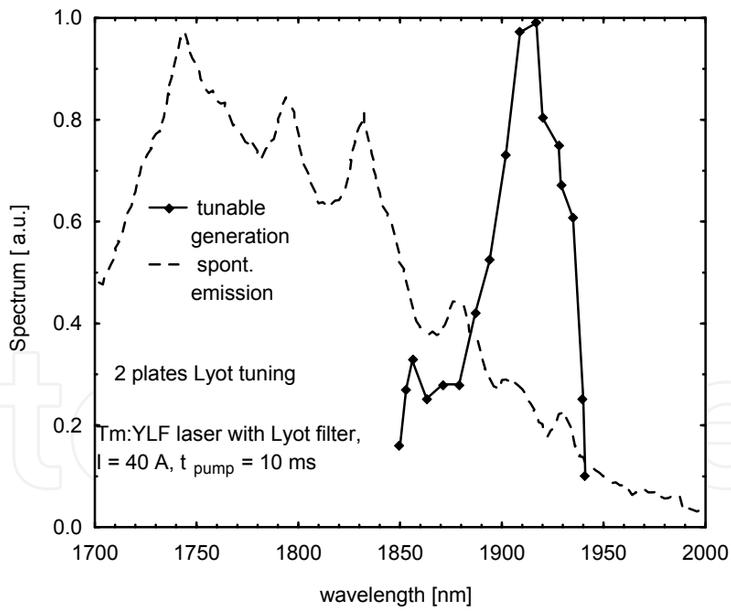

Fig. 18. Spectra of spontaneous emission and tuning of Tm:YLF laser by means of Lyot's filter.

The experiments of tuning were carried out firstly in a free-running regime. The tuning range of 1845-1935 nm was demonstrated for 37° – 47° angle of rotation with respect to the fast axis of quartz plates (see Fig. 18). The linewidth was less than 1 nm. For the Q-switching regime the contrast of a deployed birefringent filter was too low to prevent oscillation on the strongest

1908-nm line. In the last part of characterisation in a free-running regime, we have measured the beam profiles in far field in the focal plane of a 500-focal length lens. The divergence angle was about 4.3 mrad and an estimated parameter $M^2 < 1.3$ for high 20-W incident pump power.

3.3 Q-switching experiments for low duty cycle pumping

For Q-switching we have used a water cooled acousto-optic modulator made of 45-mm long fused silica, operating at a radio frequency of 40.7 MHz with a maximum power of 25 W. In fact, that was the largest element of laser head which determined its size. It was shown in separate experiments that for maximum RF power of the acousto-optic modulator the diffraction efficiency was higher than 80%, diffraction angle was about 7 mrad and the falling edge, i.e. switch off time was about 100 ns.

In the first part of the Q-switching experiments we have estimated the maximum available output energy in free-running for which the acousto-optic modulator can hold off oscillations for a switch on state of RF power. It should be noted that we have used a 220-mm long cavity with Lyot's filter inside introducing additional insertion losses. The laser output was horizontally polarized (perpendicularly to the c-axis of YLF crystal).

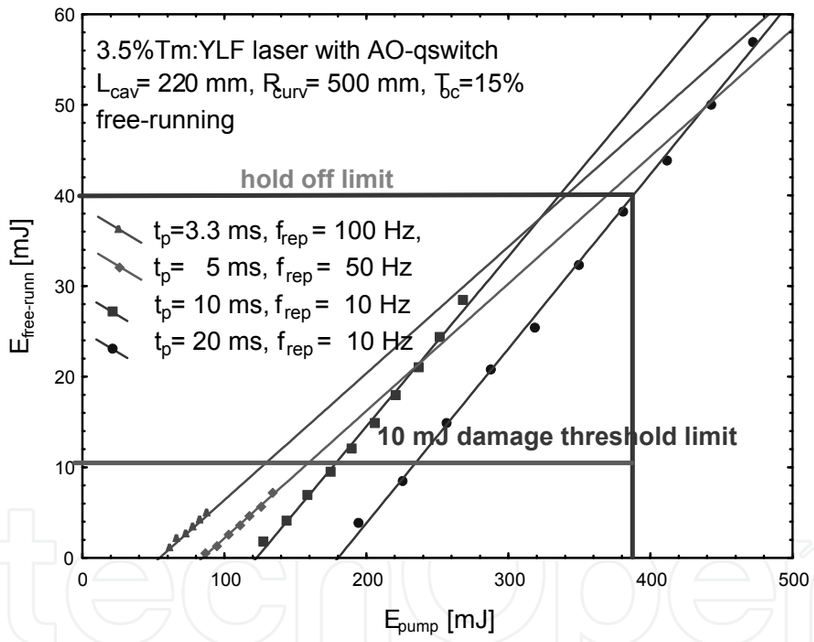

Fig. 19. Available output energy vs. incident pump energy in free running for the state of effective operation of the active Q-switch

As was shown in Fig. 19, for the best case the output energy of 40 mJ (for incident pump energy of 400 mJ) was the upper limit of efficient operation of the Q-switch. However, the real limit of output energy was far lower, because of the damage threshold of the Tm:YLF crystal facet. It was shown, that the output energy above 10 mJ corresponding approximately to 1.5 – 2 GW/cm^2 of intracavity power density constitutes the upper limit of available pulse energy for the safe operation in a Q-switching regime in the case of our laser head. Thus, we can conclude that a much smaller Q-switch without water cooling will be satisfactory for our purposes.

The results of measurements of pulse duration and peak power for a low duty cycle of 10% (10 Hz of PRF and 10 ms pump duration) were shown in Fig. 20. The shortest pulse of 22-ns duration (see Fig. 21) and 10.5 mJ energy corresponding to 0.45 MW of peak power were demonstrated for the best case of stable output below the risk of damages to laser elements.

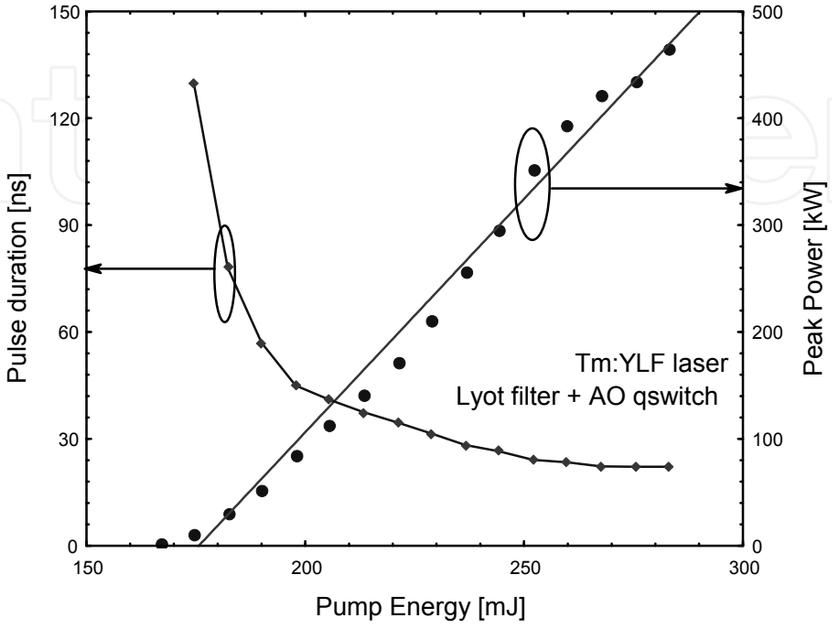

Fig. 20. Pulse duration, peak power vs. pump energy for Q-switching in a low 10% duty cycle pumping regime.

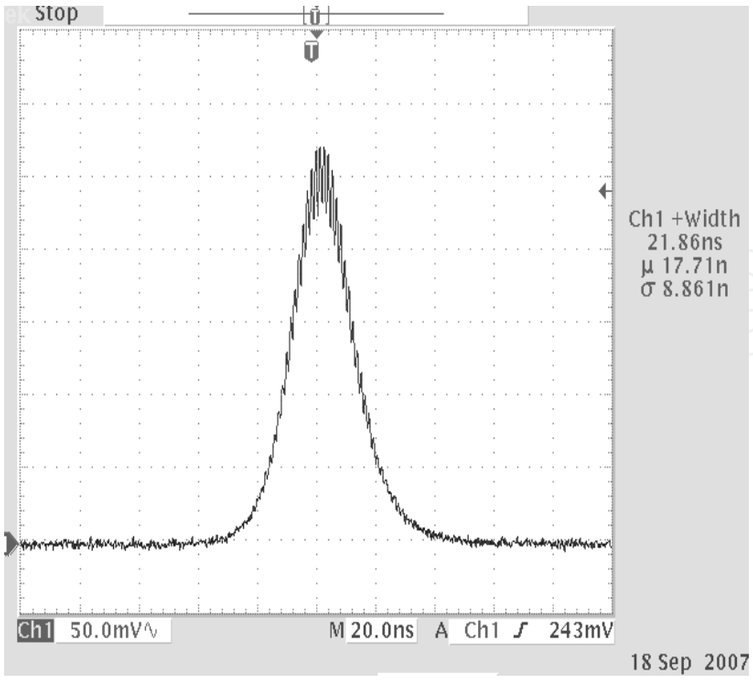

Fig. 21. Oscillogram of the giant pulse of 10.5 mJ of energy.

3.4 Q-switching experiments for CW pumping

For the CW pumping regime the maximum pump power was constituted due to the thermal lensing limit. Because of negative thermal dispersion of Tm:YLF the cavity achieves stability limit for nearly 20-W of incident pump power.

The results of the Q-switching experiments were shown in Fig. 22, 23, and collected in Table 2. Nearly 20% slope efficiency with respect to absorbed pump energy was obtained for high repetition frequency. The experimental results were in agreement with the numerical model presented in p. 2.3.2

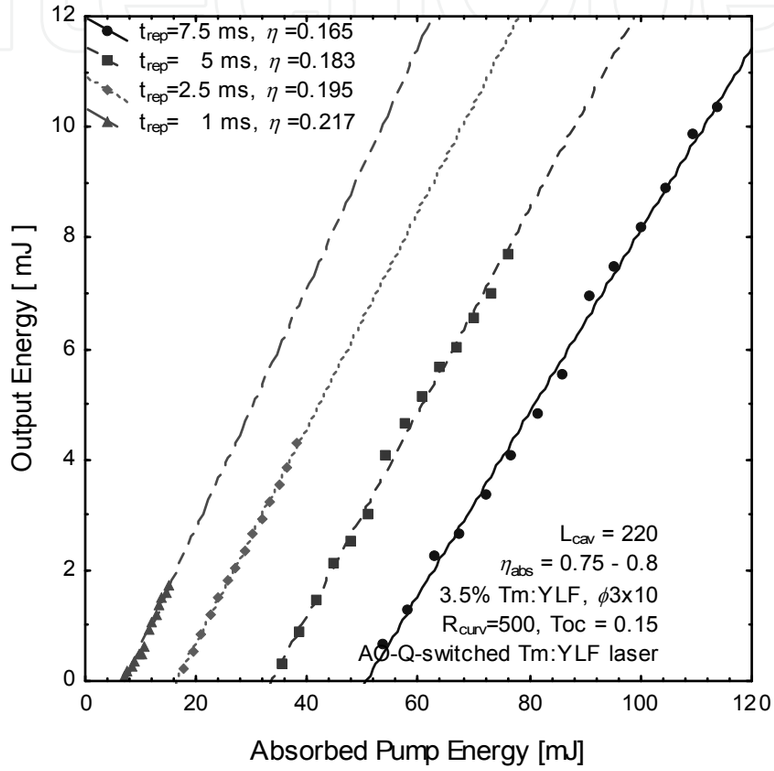

Fig. 22. Output energy vs. absorbed pump energy for different repetition periods.

f_{rep} [Hz]	d.f.	P_{avg} [W]	E_p [mJ]	τ_p [ns]	P_p [kW]
1000	1	1.725	1.725	146	11.8
400	1	1.725	4.31	101	42.7
200	1	1.541	7.7	70	110
133	1	1.38	10.35	46.8	221
10	0.1	0.105	10.5	22	447

Table 2. Results of Q-switching experiments; f_{rep} – pulse repetition frequency, d.f. – duty cycle factor, P_{avg} – average output power, E_p – pulse energy, τ_p – pulse duration, P_p – peak power.

The comparable pulse energies of 10 mJ (last two rows of Table 2) were achieved for both cases of pumping. The much longer pulse duration for a case of CW pumping was caused

by the combined effect of an increase in reabsorption and additional diffraction loss (see p. 2.3.2). Please note, that maximum available pulse energy was limited in both cases by reaching the damage thresholds of the rod facet or rear mirror.

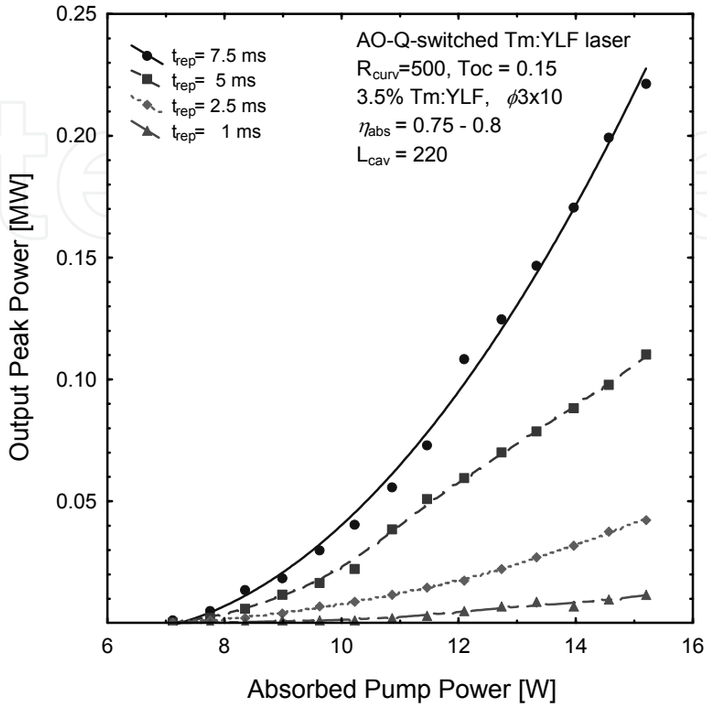

Fig. 23. Output peak power vs. absorbed pump power for different repetition periods.

4. Conclusions

The analytical models of quasi-three-level lasers operating in free running and Q-switching regimes were presented. In both cases appropriate formulae enabling the optimization of such lasers were given and analysed. The numerical model of a quasi-three-level laser operating in a Q-switching regime including additional pump dependent losses, was elaborated to explain the properties of the developed actively Q-switched laser. The main difference in analysis of Q-switching in a quasi-three-level laser (compared to a four-level laser) consists of the effect of temperature on giant pulse parameters. Because of increase in temperature with pump power, the net inversion, additional reabsorption and diffraction losses significantly influence available pulse energy, peak power and pulse duration. The all above mentioned effects result in the fact, that giant pulse is generated for a considerable level of losses dependent on effective average heat power dissipated in the gain medium. The results of numerical modelling were confirmed in the experiments.

To compare models with experiments we have presented the results of investigations of an efficient Tm:YLF laser end-pumped by 30-W fiber coupled laser diode bar. The incident pump density exceeded above 5 times the saturation pump density, thus the drawbacks of the quasi-three-level scheme have been mitigated. We have obtained the best output characteristics (slope and maximum power) for out-coupling losses of 20% evidencing the high roundtrip gain for maximum pump power. Above 7-W of output power for incident

26-W pump power in free running regime was achieved in the best case for a short 70-mm cavity. Above 3 W of output power was demonstrated for CW pumping for an elongated 220-mm cavity. The divergence angle was about 4.3 mrad and estimated parameter $M^2 < 1.3$. To improve the output characteristics in a free running regime, the optimisation of pump size in the gain medium, application of a longer rod and optimised cavity design should be applied.

For the free-running and Q-switching regimes the output spectrum was centred at 1908-nm with linewidth less than 6 nm. For tuning the Lyot's filter consisting of 2 quartz plates was deployed. The tuning range of 1845-1935 nm with less than 1-nm linewidth was demonstrated for the free-running regime. For the Q-switching regime the contrast of a deployed birefringent filter was too low to prevent oscillation on the strongest 1908-nm linewidth.

In the experiments on active Q-switching by means of an acousto-optic modulator, up to 10-mJ output energy was demonstrated. Output energy was limited by damage of the laser elements. Nearly 0.5 MW peak power with pulse durations of 22 ns was achieved for a 10-Hz repetition rate with 10% duty cycle of the pumping regime. The 1.7-W of average power with 12 kW peak power and 1000 Hz repetition rate was demonstrated for the CW pumping regime. The developed laser could constitute the basis for development of the tunable, Q-switched laser source operating at a 2-μm wavelength. Moreover, it could be used as a pump source for Ho:YAG and Cr:ZnSe lasers operating in a gain switching regime for the longer (> 2 μm) wavelengths.

5. Acknowledgments

This work was supported by the Polish Ministry of Science and Higher Education under projects 0T00A00330, NN515 423033, NN515 414834, NN515 345036.

6. References

Barnes, N., & De Young, R. (2009). Tm:germanate Fiber Laser for Planetary Water Vapor Atmospheric Profiling. *The Conference on Lasers and Electro-Optics (CLEO)/The International Quantum Electronics Conference (IQEC) (Optical Society of America, Washington, DC*, 2009 (p. JWA60). Optical Society of America, Washington, DC, 2009

Barry, D., Parlange, J., Li, L., Prommer, H., Cunningham, C., & Stagnitti, F. (2000). Analytical approximation for eal values of the LambertW function. *Math and Computers in Simulation* , Vol. 53, pp. 4-14

Beach, R. (1996). CW Theory of quasi-three-level end-pumped laser oscillators. *Optics Communications* , Vol. 123, pp. 385-393

Bourdet, G. (2001). New evaluation of ytterbium-doped materials for CW laser applications. *Optics Communications* , Vol. 198, pp. 411-417

Bourdet, G. (2000). Theoretical investigation of quasi-three-level longitudinally pumped continuous wave lasers. *Applied Optics* , Vol. 39, pp. 966-971.

Budni, P., Lemons, M., Mosto, J., & Chicklis, E. (2000). High-Power/High-Brightness Diode-Pumped 1.9-μm Thulium and Resonantly Pumped 2.1-μm Holmium Lasers *IEEE J. Sel. Top. Quant. Electron,* Vol. 6, No. 4, pp. 629-634

Chen, Y.-F. (1999). Design Criteria for Concentration Optimization in Scaling Diode End-Pumped lasers to High Powers: Influence of Thermal Fracture. *IEEE Journal of Quantum Electronics,* Vol. 35, pp. 234-239

Clarkson, W., Shen, D., & Sabu, J. (2006). High-power fiber-bulk hybrid lasers. *Proceedings SPIE*, Vol. 6100, pp. 61000A-1-13

Degnan, J. (1989). Theory of optimally coupled Q-switched laser. *IEEE Journal of Quantum Electronics* , Vol. 25, pp. 214-220

Dergachev, A., Wall, K., & Moulton, P. (2002). A CW Side-pumped Tm:YLF Laser. *OSA TOPS, Advanced Solid State Lasers, ed. M.E. Ferman L.R. Marshall*, Vol. 68, pp. 343-346

Eichhorn, M. (2008). First investigations on an Er^{3+}:YAG SSHCL. *Appl. Phys. B* , Vol. 93, pp. 817-822

Eichhorn, M. (2008). High-Power Resonantly Diode-Pumped CW Er^{3+}:YAG Laser. *Appl. Phys. B* , Vol. *93*, pp. 773-778

Eichhorn, M. (2008). Quasi-three-level solid-sate lasers in the near and mid infrared based on trivalent rare earth ions. *Appl Phys B* , Vol. 93, pp. 269-316

Eichhorn, M., & Jackson, S. (2008). High-pulse-energy, actively Q-switched Tm^{3+} -doped silica 2 m fiber laser pumped at 792 nm. *Optics Letters* , Vol. 32, pp. 2780-2782

Eichhorn, M., & Jackson, S. (2009). High-pulse-energy, actively Q-switched Tm^{3+},Ho^{3+}-codoped silica 2 m fiber laser. *Optics Letters* , Vol. 33, pp. 1044-1046

Gaponenko, M., Denisov, I., Kisel, V., Malyarevich, A., Zhilin, A., Onushchenko, A., et al. (2008). Diode-pumped Tm:$KY(WO_4)_2$ laser passively Q-switched with PbS-doped glass. *Appl Phys B* , Vol. 93, pp. 787-791

Gapontsev, D., Platonov, N., Meleshkevich, M., Drozhzhin, A., & Sergeev, V. (2007). 415W single-mode CW thulium fiber laser in all-fiber format. *CLEO Europe, 2007*, paper. CP2-3-THU

Godard, A. (2007). Infrared (2-12 μm) solid-state laser sources: a review. *C.R. Physique* , Vol. 8, pp. 1100-1128

Gorajek, L., Jabczyński, J.K. , Zendzian, W., Kwiatkowski, J., Jelinkova, H., Sulc, J., et al. (2009). High repetition rate, tunable, Q-switched, diode pumped Tm:YLF laser. *Opto-Electronics Rev.,* Vol. 6, pp. 23-35

Grace, E., New, G., & Franch, P. (2001). Simple ABCD matrix treatment for transversely varying saturable gain. *Optics Express* , Vol. 26, pp. 1776-1778

Honea, E., Beach, R., Sutton, S., Speth, J., Mitchell, S., Skidmore, J., et al. (1997). 115-W Tm:YAG Diode-Pumped Solid-State Laser. *IEEE Journal of Quantum Electronics,* Vol. 33, pp. 1592-1600.

Huber, G., Duczynski, E., & Peterman, K. (1988). Laser pumping of Ho—Tm-, Er- doped garnet laser at room temperature. *IEEE Journal of Quantum Electronics* , Vol. 24, pp. 920-923.

Jabczyński, J., Gorajek, L., Zendzian, W., Kwiatkowski, J., Jelinkova, H., Sulc, J., et al. (2009). High repetition rate, high peak power, diode pumped Tm:YLF laser. *Laser Phys. Letters* , Vol. 6, pp. 109-112

Jabczyński, J., Kwiatkowski, J., & Zendzian, W. (2003). Modeling of beam width in passively Q-switched end-pumped laser. *Optics Express* , Vol. 11, pp. .552-559

Jabczyński, J., Zendzian, W., Kwiatkowski, J., Jelinkova, H., Sulc, J., & Nemec, M. (2007). Actively Q-switched diode pumped thulium laser. *Laser Phys. Letters* , Vol. 4, pp. 863-867

Koechner, W. (1996). *Solid-State Laser Engineering*. Springer Verlag, ISBN 3-540-60237-2, Berlin

Kudryashov, I., Katsnelson, A., Ter-Gabrielyan, N., & Dubinskii, M. (2009). Room Temperature Power Scalability of the Diode-Pumped Er:YAG Eye-Safe Laser. *CLEO-Baltimore*, paper CWA2

Lim, C., & Izawa, Y. (2002). Modeling of End-Pumped CW Quasi-Three-Lvele Lasers. *IEEE Journal of Quantum Electronics* , Vol. *38*, pp. 306-311

Lisiecki, R., Solarz, P., Dominiak-Dzik, G., Ryba-Romanowski, W., Sobczyk, M., Cerny, P., et al. (2006). Comparative optical study of thulium-doped YVO_4, $GdVO_4$, and $LuVO_4$ single crystals. *Phys. Rev. B* , Vol. 74, pp. 035103.

McComb, T., Shah, L., Sims, A., Sudesh, V., Szilagyi, J., & Richardson, ,. M. (2009). Tunable Thulium Fiber Laser System for Atmospheric Propagation Experiments. *Conference on Lasers and Electro-Optics (CLEO)/The International Quantum Electronics Conference (IQEC) (Optical Society of America, Washington, DC,* paper CthR5.

Mirov, S., Fedorov, V., Moskalev, I., & Martyshkin, D. (2007). Recent Progress in Transistion-Metal-Dped II-VI Mid-IR Lasers. *IEEE Journal of Selected Topics in Quantum Electronics* , Vol. 13, pp. 810-822

Payne, S., Chase, L., Smith, L., Kway, W., & Krupke, W. (1992). Infrared Cross-Section Measurements for Crystals Doped with Er^{3+}, Tm^{3+}, and Ho^{3+}. *IEEE Journal of Quantum Electronics* , Vol. 28, pp. 2619-2630

Rustad, G., & Stenersen, K. (1996). Modeling of Laser-Pumped Tm and Ho Lasers Accounting for Upconversion and Ground-State Depletion. *IEEE Journal of Quantum Electronics , 32*, pp. 1645-1655.

Schellhorn, M. (2008). High-power diode-pumped Tm:YLF laser. *Appl. Phys. B* , Vol. 91, pp. pp. 71-74

Schellhorn, M., Ngcobo, S., & Bollig, S. (2009). High-Power Diode-Pumped Tm:YLF slab laser. *Appl. Phys. B* , Vol. 94, pp. 195-198

Schellhorn, M., Eichhorn, M., Kieleck, C., & Hirth, A. (2007). High repetition rate mid-infrared laser source. *C. R. Physique* , Vol. 8, pp. 1151-1161

Setzler, S., Francis, M., Young, Y., Konves, J., & Chicklis, E. (2005). Resonantly pumped eyesafe erbium lasers. *IEEE J. Sel. Top. Quant. Electron* , Vol. 11, pp. 645-657

So, S., MacKenzie, J., Shepherd, D., Clarkson, W., Betterton, J., & Gorton, E. (2006). A power-scaling strategy for longitudinally diode-pumped Tm:YLF lasers. *Appl. Physics B.* , Vol. 84, pp. 389-393

Sorokina, I., & Vodopyanov, K. (2003). *Solid-State Mid-Infrared Laser Sources.*: Springer Verlag, ISBN 3-540-00621, Berlin

Zhu, X., & Jain, R. (2007). 10-W-level diode-pumped compact 2.78 μm ZBLAN fiber laser. *Opt. Letters* , Vol. 32, pp. 26-28.

Advances in Solid State Lasers Development and Applications

Edited by Mikhail Grishin

ISBN 978-953-7619-80-0
Hard cover, 630 pages
Publisher InTech
Published online 01, February, 2010
Published in print edition February, 2010

Invention of the solid-state laser has initiated the beginning of the laser era. Performance of solid-state lasers improved amazingly during five decades. Nowadays, solid-state lasers remain one of the most rapidly developing branches of laser science and become an increasingly important tool for modern technology. This book represents a selection of chapters exhibiting various investigation directions in the field of solid-state lasers and the cutting edge of related applications. The materials are contributed by leading researchers and each chapter represents a comprehensive study reflecting advances in modern laser physics. Considered topics are intended to meet the needs of both specialists in laser system design and those who use laser techniques in fundamental science and applied research. This book is the result of efforts of experts from different countries. I would like to acknowledge the authors for their contribution to the book. I also wish to acknowledge Vedran Kordic for indispensable technical assistance in the book preparation and publishing.

How to reference

In order to correctly reference this scholarly work, feel free to copy and paste the following:

Jan K. Jabczynski, Lukasz Gorajek, Waldemar Zendzian, Jacek Kwiatkowski, Helena Jelinkova, Jan Sulc and Michal Nemec (2010). Actively Q-switched Thulium Lasers, Advances in Solid State Lasers Development and Applications, Mikhail Grishin (Ed.), ISBN: 978-953-7619-80-0, InTech, Available from: http://www.intechopen.com/books/advances-in-solid-state-lasers-development-and-applications/actively-q-switched-thulium-lasers

INTECH
open science | open minds

InTech Europe
University Campus STeP Ri
Slavka Krautzeka 83/A
51000 Rijeka, Croatia
Phone: +385 (51) 770 447
Fax: +385 (51) 686 166
www.intechopen.com

InTech China
Unit 405, Office Block, Hotel Equatorial Shanghai
No.65, Yan An Road (West), Shanghai, 200040, China
中国上海市延安西路65号上海国际贵都大饭店办公楼405单元
Phone: +86-21-62489820
Fax: +86-21-62489821

© 2010 The Author(s). Licensee IntechOpen. This chapter is distributed under the terms of the Creative Commons Attribution-NonCommercial-ShareAlike-3.0 License, which permits use, distribution and reproduction for non-commercial purposes, provided the original is properly cited and derivative works building on this content are distributed under the same license.

IntechOpen

IntechOpen